ISBN: 978-3-95450-231-8 ISSN: 2673-5490 doi: 10.18429/JACoW-IPAC2023-TUPM101

MUTUAL INTERACTION OF 2 M LONG ELECTRON PLASMA ENSEMBLES WITH AN ION BEAM IN MEV RANGE

K I. Thoma*, M. Droba, O. Meusel
Goethe Universität Frankfurt am Main, Germany

Abstract

Gabor-lens 2000 (GL2000) is an hadron optic device which confines a 2 m long electron cloud. This opens up new possibilities in research with very long confined static electron ensembles. Due to the optimization of technical design it was possible to successfully complete the conditioning process creating a stable confinement of electrons. Also, the diagnostic tools were extended and the control and measurements was automated. This made it possible to scan a large parameter space with varying the external confinement parameters magnetic field, potential and residual gas pressure. In addition, numerical models of GL2000 confinement parameters were simulated to derive the operation function for different production and loss mechanisms at different potential and magnetic field settings. This should make it possible to adjust the particle ensemble within the Gabor-lens (GL) in a way, that the plasma state is defined. For applications of GLs in transport channels, particle accelerators or final focus sections it is than possible to create a perfect linear mapping of the beam and therefore a smooth focusing with space charge compensation. Using the TraceWin tool, simulations were made for beam transport through high energy beam transport lines. In addition, GL2000 was implemented to the Van-de-Graaf beamline at IKF[1], to be able to investigate beam-cloud interactions and perform first transport measurements.

INTRODUCTION

The confinement of electrons in the Gabor-lens [1] is radially created by an axial magnetic field, which is made by a solenoid configuration. The longitudinal confinement is given by a potential well, between the anode tube and the electrode system on each side. The resulting positive electric field accelerates electrons inside the lens. The initial electron is generated by various physical processes, for example, background radiation. It gets accelerated and produces more electrons by residual gas ionisation. At some point an avalanche effect sets in, the electron cloud is created. A Gabor-lens does not need any external source for electron production, the electron cloud is a non-neutral plasma and fullfills plasma criteria for collective behavior [2].

With GL2000 introduced in [3] a large number of experiments could be performed due to technical improvements and automation processes in the measurement routine in addition to numerical calculations and simulations.

The aim of the study was first to run a large parameter space with different settings of external confinement parameters, both on the experiment itself and in the numerical calculations. The experimental data includes the homogeneous confinement of the lens on its operation function [3] as well as the non-homogeneous region. With the results, it should now be possible to better assess the performance of the lens and to precisely adjust its focusing properties.

For the use of the lens in high energy beamlines these results are essential to guarantee a linear mapping of the ion beam and thus not only to compensate the space charge but also to reach a smooth focusing of the ion beam and to increase the luminosity on the target of the respective experiments. The measurement data of GL2000 beyond its operation function and homogeneous confinement, however, also opens up new possibilities for physics with Gabor-lenses.

EXPERIMENTAL DATA

Experimental data were collected in the following parameter range:

- Potential Φ_A: 0-20 kV
- Magnetic field B_z: 0-18 mT
- Residual gas pressure p_{RGA}: 8×10^{-8} mbar - 5×10^{-6} mbar

The measurements were divided into large, coarser scans in which almost the entire parameter space currently available was measured. These measurements were each repeated at different residual gas pressures, up to the point where no more residual gas was admitted into the volume of the lens. Furthermore, the measurements were divided into deep scans, in which small areas were traversed very precisely and this was repeated several times. In these first series of measurements, power supply current, as well as the current of particles hitting an installed Faraday cup, were measured. The current measured at the power supply I_{total} and Faraday cup I_{FDC} is defined as follows:

$$I_{total} = I_{ion} + Ie, \quad (1)$$

$$I_{FDC} = I_{ion}/2. \quad (2)$$

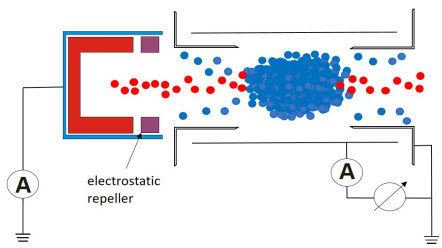

Figure 1: Electron production: RGA + e -> RGI + 2e.

* thoma@iap.uni-frankfurt.de
[1] Institute for Nuclear Physics, Goethe-University Frankfurt

Content from this work may be used under the terms of the CC BY 4.0 licence (© 2022). Any distribution of this work must maintain attribution to the author(s), title of the work, publisher, and DOI.

ISBN: 978-3-95450-231-8 ISSN: 2673-5490 doi: 10.18429/JACoW-IPAC2023-TUPM101

© Content from this work may be used under the terms of the CC BY 4.0 licence (© 2022). Any distribution of this work must maintain attribution to the author(s), title of the work, publisher, and DOI.

Parameter Space Scan

Figure 2 (a) shows such a parameter space scan at a residual helium gas pressure of 7×10^{-6} mbar. The three plotted curves (yellow, red, green) represent the theoretically calculated operation function, each with a slightly adjusted gradient.The blue lines mark the values 9, 12 and 18 mT and represent the numerical data used in Fig. 3.

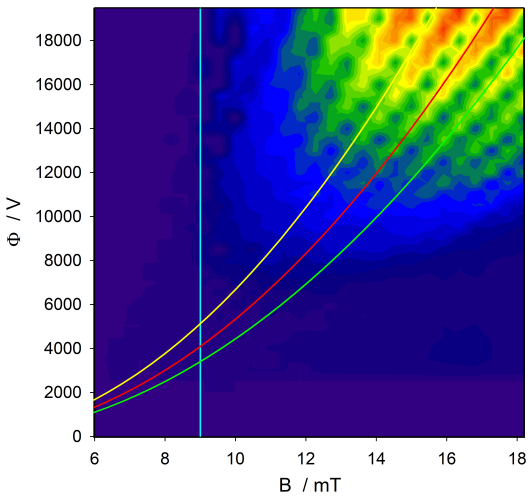

(a) Parameter space scan of GL2000, residual gas pressure: $7 \cdot 10^{-6}$ mbar

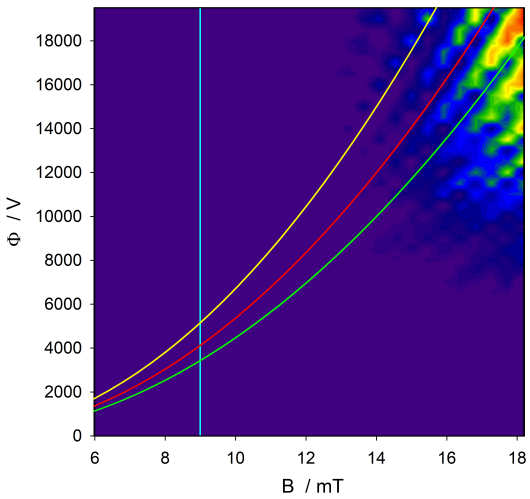

(b) Parameter space scan of GL2000, residual gas pressure: $5.5 \cdot 10^{-7}$ mbar, same parameter space, different residual gas pressures as shown in (a)

Figure 2: Comparison of two parameter space scans with identical external parameters but different residual gas pressure.

The color code is related to the total current I_{total}. It shows that the intensity increases with increasing external parameters, but also that this does not happen uniformly. The micro structure consists of peaks and valleys forming a pattern in the intensity of I_{total} measured by the power supply. A similar result can also be stated for the measured Faraday cup current I_{FDC}. Both results indicate a behavior of the electron density which was not observed so far.

When varying the residual gas pressure, the production rate of electrons and ions in the lens volume changes, as well as their loss rate. This is clearly visible in figure 2 (b). The overall intensity of the current measured at the power supply decreases and the pattern is shifted with respect to the operation functions.

All three external parameters (Φ_A, B_z, p_{RGA}) have an impact on the performance of the lens and change its properties as focusing device. Depending on the electric potential and the magnetic field, the performance of the lens is on or beside the operation function, so the mapping is linear or not. This is because the density profile inside the lens is changing from homogeneous to Gauß or hollow-profile, which is presented in the numerical part of the paper. As a result, confinement and residual gas pressure have to be taken into account for adjusting density and density distribution. This was studied numerically.

NUMERICAL SIMULATIONS OF ELECTRONS INSIDE THE LENS

The self-consistent code GABORM was used to simulate the parameter space scan with the variation in magnetic field and electric potential similar to the experiment.The code enables the possibility to adjust a production rate and loss rate of electrons. Both parameter deliver a thermal state of the electron column. For this purpose, the parameters production rate $\Delta n_e[C/m^{-3}]$ and loss current $I_{loss}[A]$ were varied while the magnetic field B_z and the electric potential Φ_A were kept constant. The production rate is represented by the increase of the density Δn_e per cell and iteration step [4].

Parameter Space Scan Numerical Experiment

In Fig. 3 the comparison of the normalized data between experiment and simulation is shown for a B-field of 9 mT (according to the blue line in Fig.2). The settings for the

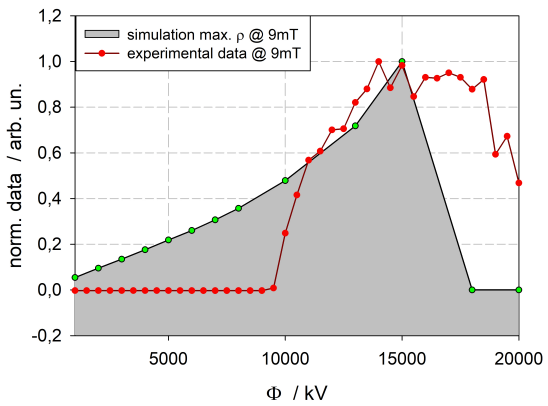

Figure 3: Comparison of the normalized data between experiment and simulation.

ISBN: 978-3-95450-231-8 ISSN: 2673-5490 doi: 10.18429/JACoW-IPAC2023-TUPM101

simulations were: I_{loss} = 1A and $DF = 5 \times 10^{-5}$C/m^{-3}. This parameters were chosen because previous numerical studies have shown that the ratio of mean and maximum density $< n_e > /n_{e,max}$ is nearly one for this case. It can be seen in Fig.3 that both the measured power supply current as well as the the density in the simulation increase as the potential increase. At 15 kV, the simulated electron density decreases, no confinement of electrons is predicted by the numerical model. In the experiment, a decrease can also be seen, but it is shifted to higher anode voltages. Unfortunately the maximum voltage was limited to 20 kV because of the risk of sparking.

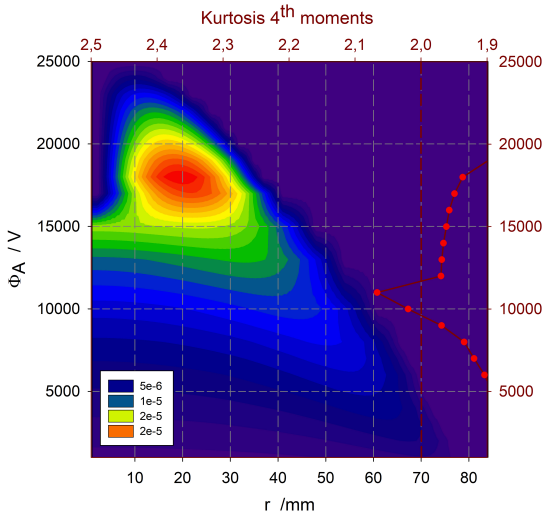

Figure 4: $\rho(r)$ as a function of Φ_A for Bz = const.

Figure 4 shows the density profiles $n_e(r)$ in the center of the GL as a function of Φ_A for a given magnetic field. The radius of the cloud as well as a variation of the density distribution depends on Φ_A. This can be recognized mathematically by the use of the kurtosis, the fourth momenta. The kurtosis is related to the fourth-order and second-order moments, defined as:

$$K = \frac{\langle x^4 \rangle}{(\langle x^2 \rangle)^2} \tag{3}$$

For the two-dimensional case of the radial symmetric profiles in this case, a transformation from x into r, φ coordinates is made. A homogeneous distribution applies for:

$$\langle x^2 \rangle = \frac{\int_0^{2\pi}\int_0^{R_{max}} r^2 cos^2(\varphi) r dr d\varphi}{\int_0^{2\pi}\int_0^{R_{max}} r dr d\varphi} = \frac{\frac{1}{2}\cdot 2\pi \cdot \frac{R_{max}^4}{4}}{2\pi \cdot \frac{R_{max}^2}{2}} = \frac{R_{max}^2}{4} \tag{4}$$

$$\langle x^4 \rangle = \frac{\int_0^{2\pi}\int_0^{R_{max}} r^4 cos^4(\varphi) r dr d\varphi}{\int_0^{2\pi}\int_0^{R_{max}} r dr d\varphi} = \frac{\frac{3}{4}\cdot \pi \cdot \frac{R_{max}^6}{6}}{2\pi \cdot \frac{R_{max}^2}{2}} = \frac{R_{max}^4}{8} \tag{5}$$

$$\Rightarrow \frac{\langle x^4 \rangle}{(\langle x^2 \rangle)^2} = \frac{\frac{R_{max}^4}{8}}{(\frac{R_{max}^2}{4})^2} = \underline{2} \tag{6}$$

For a numeric calculation of the radial profiles Eq. (6) is generalized to:

$$\frac{\langle x^4 \rangle}{\langle x^2 \rangle^2} = \frac{3}{2}\frac{\sum i^5 n_i \cdot \sum i \cdot n_i}{(\sum n_i \cdot i^3)^2}. \tag{7}$$

Figure 4 shows $K(\Phi_A)$ in the midplane of the lens. The density distribution changes as a function of Φ_A.

GABOR-LENS FOR BEAM TRANSPORT

In collaboration with CERN and GSI, simulations have been made using GLs for space charge compensation and beam focusing in transport channels and accelerator facilities in addition to existing beam optics. The different electron density distributions and the resulting self-fields were transformed in drift-kick-matrices for the implementation in TraceWin code. This enables a detail study of the beam dynamics for linear and non-linear focusing forces. GL2000 was connected to a Van-de-Graaf accelerator at the IKF to perform first pre-experiments with beam using He^+, H^+ and Xe^+ beams in an energy range of 0.5-2 MeV [5], [6].

First Transport Experiments

The resent results of GL experiments show a dependence of the density distribution from residual gas pressure for a given confinement. To investigate the radial shape of the electron column and the ion beam passing the Gabor-lens at the same time an optical diagnostic was tested. A ccd-camera was mounted at the end of the beam line, right behind a vacuum window. The beam was stopped by a quartz glass. Passing a rectangular aperture the beam produced a rectangular gleam on the glass see Fig. 5 (left). When the Gabor-lens is switched on, the confined electrons induce a fluorescence of the residual gas. The electron density distribution can be observed through the quartz window under the assumption of a homogeneous residual gas distribution in superposition of the beam-induced gleam as shown in Fig. 5 (right).

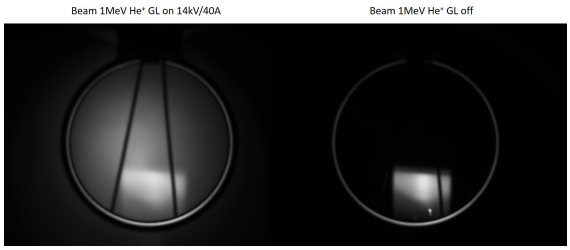

Figure 5: superposition of residual gas fluorescence induced by the electron column and beam induced gleam on the quartz window (left) and signal of the beam without electron confinement in the Gabor-lens (right).

ACKNOWLEDGMENTS

We express our thanks to the technical staff of IKF for the excellent support of our experimental campaign.

Content from this work may be used under the terms of the CC BY 4.0 licence (© 2022). Any distribution of this work must maintain attribution to the author(s), title of the work, publisher, and DOI.

ISBN: 978-3-95450-231-8 ISSN: 2673-5490 doi: 10.18429/JACoW-IPAC2023-TUPM101

© Content from this work may be used under the terms of the CC BY 4.0 licence (© 2022). Any distribution of this work must maintain attribution to the author(s), title of the work, publisher, and DOI.

REFERENCES

[1] Dennis Gabor, "A Space-Charge Lens for the Focusing of Ion Beams", *Nature*, vol. 19, July 1947.

[2] Oliver Meusel, "Focussing and transport of ion beams using space charge lenses", Goethe University, Frankfurt a. M., Germany, 2005.

[3] K. I. Thoma, M. Droba, O. Meusel, "Investigation, simulation and first measurements of a 2m long electron column trapped in a gabor-lens device", *J. Phys. Conf. Ser.*, IOP Publishing, vol. 2420, p. 012042, 2023. doi:10.1088/1742-6596/2420/1/012042

[4] Jürgen Pozimski and Oliver Meusel, "Space charge lenses for particle beams", *Rev. Sci. Instrum.*, vol. 76, p. 063308, 2005. doi:10.1063/1.1904203

[5] A. Sherjan, M. Droba, O. Meusel, S. Reimann, and K. I. Thoma, "Beam Transport Simulations Through Final Focus High Energy Transport Lines with Implemented Gabor Lenses", in *Proc. IPAC'22*, Bangkok, Thailand, Jun. 2022, pp. 663–666. doi:10.18429/JACoW-IPAC2022-MOPOMS017

[6] K. I. Thoma, M. Droba, O. Geithner, M. Heilmann, C. Hessler, O. Meusel, H. Podlech, S. Reimann, P. Schuett, A. Sherjan, "Improvement of Beam Transport in High Energy Transfer Lines using Gabor-lenses", presented at the IPAC'23, Venice, Italy, May 2023, paper TUPM102, this conference.